

# Design and Analysis of Minkowskized Hybrid Fractal Like Antenna for Multiband Operation

Binod K. Soni<sup>1, \*</sup> and Rakesh Singhai<sup>2</sup>

**Abstract**—A hybrid Minkowskized fractal-like antenna structure for wireless application is presented in this paper. The Minkowskized radiating structure and feed line have been designed at the top layer of the FR-4 substrate ( $\tan(\delta) = 0.02$ ,  $\epsilon_r = 4.3$ ,  $h = 1.6$ ). A modified ground plane with a parasitic patch is etched at the bottom side of the dielectric substrate. The fabricated antenna exhibits the resonance at frequencies 0.83, 1.05, 1.6, 2.12, 3.25, 3.75 and 5.2 GHz. It covers six bands of frequencies band-1 (0.825–0.835 GHz), band-2 (0.913–1.22 GHz), band-3 (1.33–1.79 GHz) band-4 (2.04–2.18 GHz) band-5 (2.9–3.91 GHz) and band-6 (4.9–5.64 GHz) for  $|S_{11}| \leq -10$  dB which are suitable for several wireless communication bands (i.e., GSM 900 MHz, 1800 MHz, Wi-MAX, Wi-Fi 802.11y and WLAN 802.11b/g/a). The surface current distribution and radiation pattern have been studied at resonating frequencies.

## 1. INTRODUCTION

The need for compact wideband and multi-band antennas with low profile features is growing in the wireless industry. Therefore, the primary concern of the researcher is to design high performance, multi-band, compact size, and wideband antennas. An introduction of the fractal antenna presented in [1–3] supports researchers to the great extent in this context. In 1975 Mandelbrot [4] introduced the term fractal which is a fragmented or rough geometrical shape which can be subdivided into several parts, where each part is a diminished copy of the entire structure. In the year 1995, Cohen [5] elaborated the concept of fractal antenna as an introductory scientific publication. He explained the concept of a fractal and fractals abilities to reduce the size of an antenna without compromising its performance. Since then, various research concepts [6–15] related to fractal antenna have been revealed, and a new era of fractal antenna theory has begun. Various fractal antennas such as Sierpinski triangle [19], Koch dipole, meander and Minkowski fractal [16, 17] show the advantages of fractal geometry over the popular fractal Sierpinski and Koch curve and become references. In [16] Minkowski boundary fractal antenna was designed for wideband operation. Paper [17] presented a CPW-fed slot antenna with a dielectric resonator for Heptaband operation. The study revealed that Koch curve dipole reduced the size of an antenna in comparison with the regular dipole antenna and affect resonant frequency in a positive way [9]. Also, Sierpinski triangle which is popularly known as Sierpinski gasket shows multi-band behavior with growing number of iterations. Such type of antenna shows similar behavior with respect of return loss characteristics and radiation pattern at multiple frequencies of operation and is most popular for consideration. Paper [18] presented another fractal geometry known as Van Koch monopole fractal antenna with improved radiation resistance and bandwidth. Several hybrid fractal or fractal-like structures have been designed and explained for multi-band applications [20, 21, 29, 30]. Papers [27, 28] reported a combination of two popular fractals, Sierpinski and Koch, in superior-inferior manner. The proposed multifractal antennas in these articles proved their superiority and advantage

---

Received 29 September 2018, Accepted 12 November 2018, Scheduled 14 December 2018

\* Corresponding author: Binod Kumar Soni (sonibs1978@gmail.com).

<sup>1</sup> UIT RGPV, Bhopal, India. <sup>2</sup> RGPV, Bhopal, India.

over monofractal. In addition, novel heterostructures and two-dimensional materials which explored optoelectronics and photonic properties have increased the possibility to employ semiconductor material for detection electromagnetic radiations at Terahertz frequencies [22–24]. The coupling of optoelectronic devices to the antenna reported in [25, 26] may shift the operating frequency bands from GHz to THz.

In this communication, a novel hybrid fractal structure is designed, which exhibits multiple resonating frequencies such as 0.83, 1.05, 1.6, 2.12, 3.25, 3.75 and 5.2 GHz. The proposed structure covers six frequency bands: band-1 (0.825–0.835 GHz), band-2 (0.913–1.22 GHz), band-3 (1.33–1.79 GHz) band-4 (2.04–2.18 GHz) band-5 (2.9–3.91 GHz) and band-6 (4.9–5.64 GHz) which are suitable for GSM 900 MHz, 1800 MHz, Wi-MAX, Wi-Fi 802.11y and WLAN 802.11b/g/a wireless communication services. Organization of this communication is summarized as below.

Section 2 provides dimensional detail of the proposed geometry. The comparison between various iterations of the antenna is presented in Section 3. Measured and simulated results for validation of the design and analysis are presented in Section 4. The surface current distribution and radiation pattern are also discussed in Sections 5 and 6.

## 2. ANTENNA CONFIGURATION

The two-dimensional planner geometry of the proposed antenna ( $L \times W$ ) with parameters is displayed in Figure 1 which is placed on the  $Z = 0$  plane. A  $50 \Omega$  microstrip feed line ( $M_1 \times M_2$ ) is designed on the top layer of an FR-4 substrate ( $\tan(\delta) = 0.02$ ,  $\epsilon_r = 4.3$  and  $h = 1.6$  mm) which is terminated on the vertex of the isosceles triangle connecting two equal arms of 20 mm each.

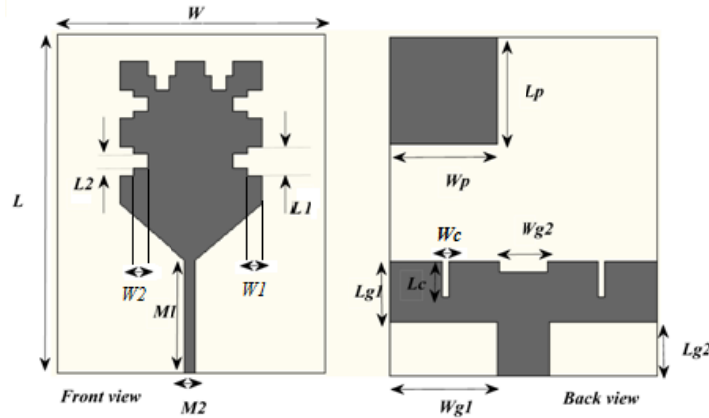


**Figure 1.** Geometry of the Minkowskized hybrid fractal like antenna.

This isosceles triangle at the third arm of 40 mm is Boolean added to a square-shaped element with the size of  $40 \times 40 \text{ mm}^2$ . This Boolean addition forms a nonuniform pentagon, which is iterated with the dimension  $L_1$ ,  $W_1$ ,  $L_2$  and  $W_2$  in Minkowski manner. On the other side of the substrate, the ground plane is etched with the parameters of  $L_{g1}$ ,  $W_{g1}$ ,  $L_{g2}$  and  $W_{g2}$ . Two rectangle-shaped symmetric slots ( $L_c \times W_c$ ) are embedded in top edge of the ground plane. The optimized values of  $L_c$  and  $W_c$  for better impedance matching are shown in Table 1. A rectangle-shaped parasitic element ( $L_p \times W_p$ ) is integrated at the top left corner of the ground plane. The optimized dimensions of the proposed antenna are presented in Table 1.

## 3. EVOLUTION OF ANTENNA

The evolution of the proposed Minkowskized hybrid fractal-like antenna is illustrated in Figure 2. A comparative graph of iterations 1, 2 and 3 is depicted in Figure 3. Antenna 1 (iteration 0) contains a simple pentagon-shaped radiating element, feed structure, parasitic element, and deformed ground plane.

**Table 1.** Optimized dimension of proposed antenna.

Parameter	Dimension (mm)	Parameter	Dimension (mm)
$M_1$	32.5	$L_1$	8
$M_2$	3	$L_2$	4
$L_{g1}$	17.5	$W_{g2}$	14
$W_{g1}$	30	$L_{g2}$	15
$W$	75	$L_c$	10
$L$	90	$W_c$	2
$W_2$	4	$L_p$	30
$W_1$	4	$W_p$	30

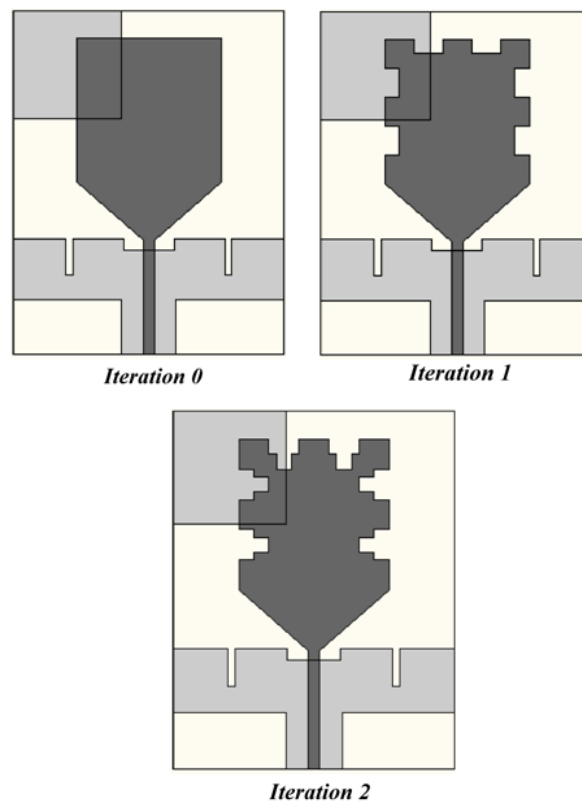


**Figure 2.** Development of Minkowskized hybrid fractal like antenna.

Antenna 1 exhibits four resonating frequencies 1.092, 1.726, 2.4 and 3.58 GHz after feeding of electromagnetic energy. Further, a Minkowski island mannered slot is introduced in non-radiating edges and an upper radiating edge of the pentagonal patch. The indentation factor, known as a ratio of width to length, is as given below,

$$i_1 = \frac{W_1}{L_1} \tag{1}$$

On optimizing slots in three sides of a nonuniform pentagon for values 0.1, 0.3, 0.5, 0.7, 0.9 and 1 as indentation factor, the optimized value of indentation factor is found as 0.5 which provides an appropriate frequency response. Antenna 2 (iteration 1) shows resonating frequencies at 1.066, 1.733, 2.418, 3.58 and 5.62 GHz. A small shift in resonating frequencies is noticed which occurs due to

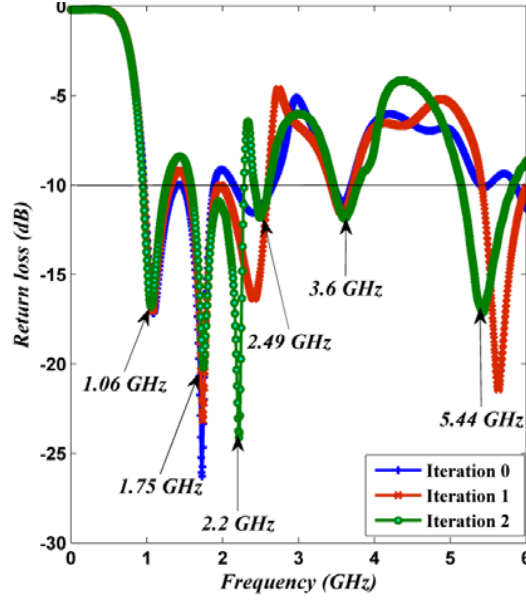


**Figure 3.** Frequency response of antenna 1, 2 and 3.

incorporation of the slot on the radiating patch. Basically, slot introduces slow wave effect and modifies the phase velocity ( $v_p = 1/\sqrt{LC}$ ) of the resonating modes. This Minkowski shape structure provides a larger perimeter to current vectors to travel around the antenna structure than the perimeter provided by antenna 1 (iteration 0). Due to this, the position of resonating frequencies is modified, and new resonant frequency, as well as band of frequency, is obtained. In the second iteration, the indentation factor is determined by an equation given below,

$$i_2 = \frac{W_2}{L_2} \quad (2)$$

The optimized value of  $i_2$  is found as 1 for  $L_2 = 4$  and  $W_2 = 4$ . Antenna 3 (iteration 2) covers the five frequency bands: band-1 (0.948–1.2534 GHz), band-2 (1.584–2.28 GHz), band-3 (2.41–2.60 GHz) band-4 (3.462–3.78 GHz) and band-5 (5.178–5.82 GHz) for  $|S_{11}| \leq -10$  dB. The corresponding fractional bandwidths of these five bands are 27.74% (band-1), 36% (band-2), 7.58% (band-3), 8.78% (band-4) and 11.67% (band-5).

#### 4. EXPERIMENTAL RESULTS

The fabricated Minkowskized hybrid fractal-like antenna is shown in Figure 4. The numerical investigation is carried out with the help of CST Microwave Studio. In the simulation, the proposed structure is excited with the help of waveguide port. After fabrication, this antenna is tested using Vector Network Analyzer Agilent Technologies N9923A in the frequency range of 0.5 to 6 GHz. Figure 5 represents the comparison between measured and simulated  $S_{11}$  characteristics. The fabricated antenna exhibits resonances at frequencies 0.83, 1.05, 1.6, 2.12, 3.25, 3.75 and 5.2 GHz. A good matching between measured and simulated  $S_{11}$  characteristics is found. However, a small error is found due to soldering effect, connector loss, and fabrication error. The fabricated antenna covers the six frequency bands. Table 2 shows a list of the covered frequency bands of the proposed antenna and their fractional bandwidth ( $BW(\%) = (f_h - f_l) * 200 / (f_h + f_l)$ ).

Figure 6 illustrates the variation of an input impedance of Minkowskized hybrid fractal-like antenna. In Smith chart, loops are inspected, which confirms the coupling between modes. In frequency band 2.9–3.91 GHz, two resonating frequencies are overlapped to each other. Due to this overlapping, a loop is formed in the Smith chart.

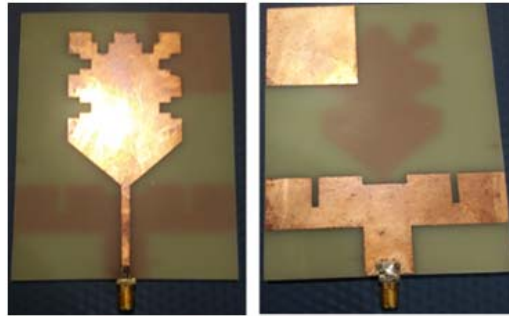


Figure 4. Fabricated Minkowskized hybrid fractal like antenna.

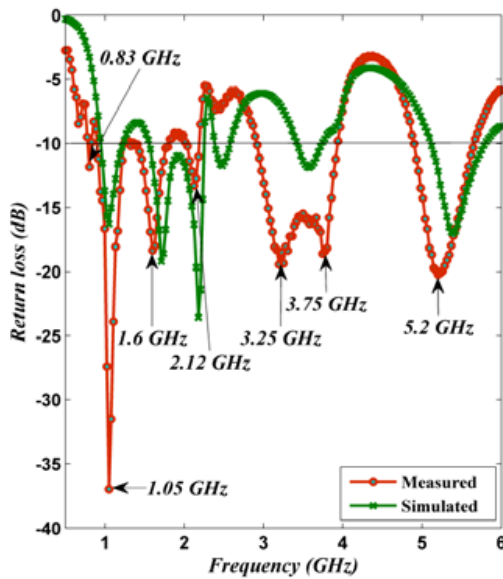


Figure 5. Measured and simulated frequency response of the proposed antenna.

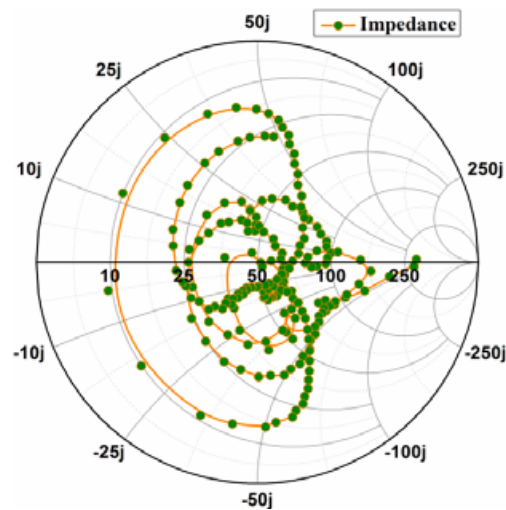


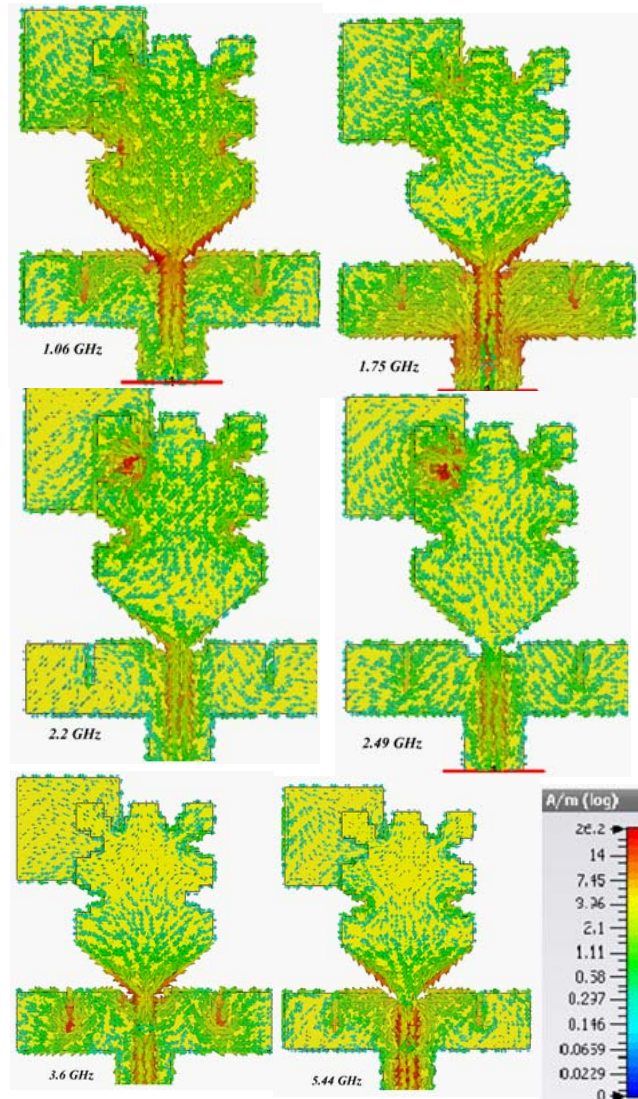
Figure 6. Variation of input impedance of Minkowskized hybrid fractal like antenna.

Table 2. Frequency response characteristic of fabricated antenna.

Frequency Band (GHz)	Measured Resonance frequency (GHz)	Bandwidth (%)
0.825–0.835	0.83	1.2
0.913–1.22	1.05	28.78
1.33–1.79	1.6	29.48
2.04–2.18	2.12	6.63
2.9–3.91	3.25, 3.75	29.66
4.9–5.64	5.2	14.04

### 5. SURFACE CURRENT DISTRIBUTION

The surface current distribution of the proposed antenna at resonating frequencies is displayed in Figure 7. At frequencies 1.06 GHz and 1.75 GHz, the current density is maximum at the bottom side of the pentagonal radiating element. In addition, at frequency 1.06 GHz, one halfwave variation of current vectors is observed on the perimeter of the radiating element whereas two half wave variations



**Figure 7.** Surface Current Distribution at resonating frequencies 1.06, 1.75, 2.2, 2.49, 3.6 and 5.4 GHz.

are inspected at frequency 1.75 GHz.

At frequencies 2.2 and 2.49 GHz, the current density is observed maximum at the top left side of the radiating patch. It is noticed that as frequency increases the number of modes is also increased. At frequencies 3.6 and 5.44 GHz, a complicated surface current distribution is noticed.

## 6. FAR FIELD PATTERN

The simulated far-field pattern is depicted in Figure 8 and Figure 9. At frequency 1.06 GHz, eight-shaped patterns are found in  $E$  plane. At higher frequencies (3.6 and 5.44 GHz), the pattern is deformed due to the presence of higher order modes. At frequencies 1.75, 2.2 and 2.49 GHz, partial eight-shaped patterns are investigated.

At frequency 1.06 GHz, we notice an omnidirectional pattern. At frequencies 1.75, 2.22 and 2.49 GHz, a partial omnidirectional pattern is found. Due to the existence of higher order modes, the omnidirectionality is lost at frequencies 3.6 and 5.44 GHz, and deformed pattern like a butterfly are observed.

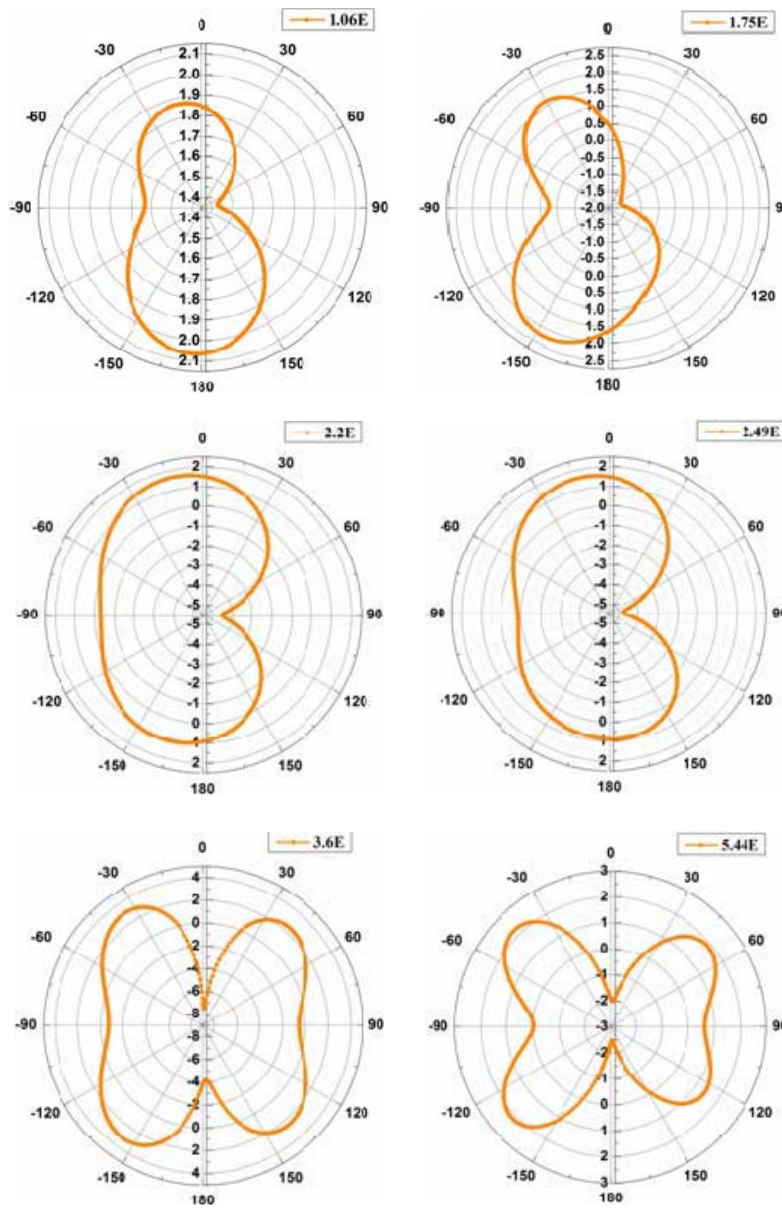
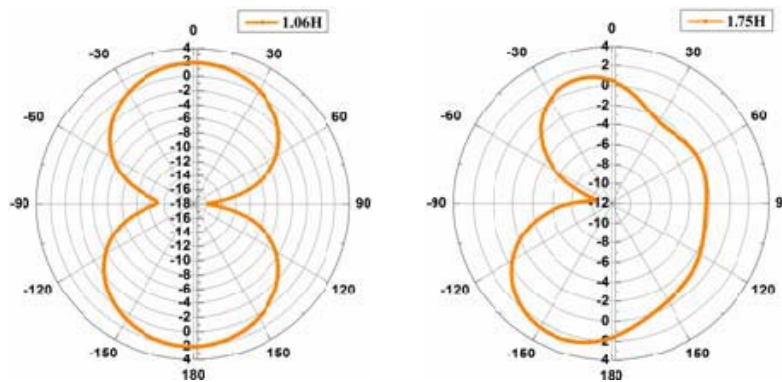
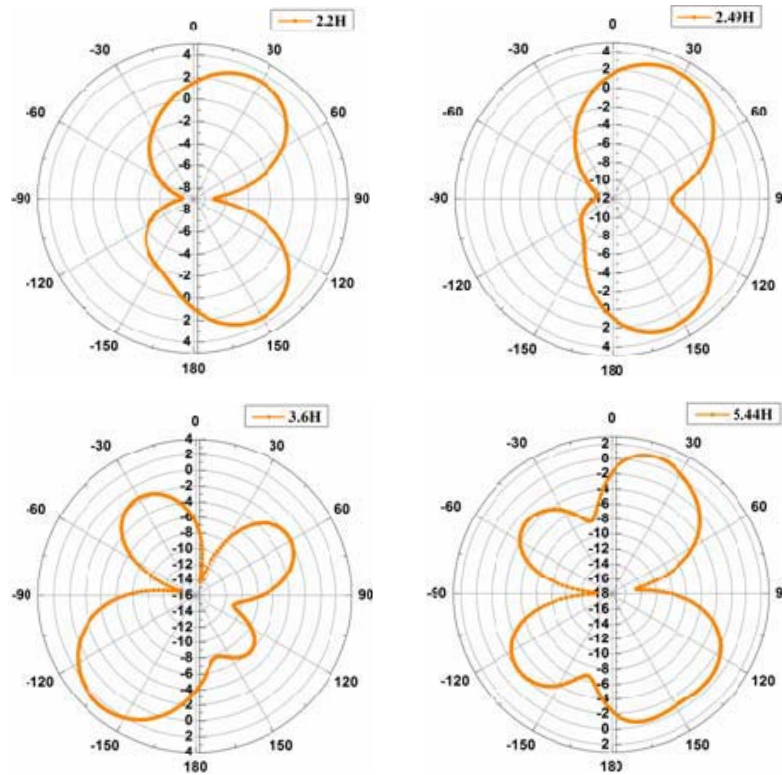


Figure 8. E-Plane pattern resonating frequencies 1.06, 1.75, 2.2, 2.49, 3.6 and 5.4 GHz.





**Figure 9.**  $H$ -Plane pattern resonating frequencies 1.06, 1.75, 2.2, 2.49, 3.6 and 5.4 GHz.

## 7. CONCLUSION

A Minkowskized hybrid fractal-like multiband antenna has been simulated and fabricated. Multi-frequency operation is achieved using iteration method of fractal antenna. This fabricated antenna exhibits resonances at frequencies 0.83, 1.05, 1.6, 2.12, 3.25, 3.75 and 5.2 GHz. It has covered six bands of frequencies band-1 (0.825–0.835 GHz), band-2 (0.913–1.22 GHz), band-3 (1.33–1.79 GHz) band-4 (2.04–2.18 GHz) band-5 (2.9–3.91 GHz) and band-6 (4.9–5.64 GHz) for  $|S_{11}| \leq -10$  dB which are suitable for several wireless communication bands (i.e., GSM 900 MHz, 1800 MHz, Wi-MAX, Wi-Fi 802.11y and WLAN 802.11b/g/a).

## REFERENCES

1. Werner, D. H. and S. Ganguly, "An overview of fractal antenna engineering research," *IEEE Antennas Propagation Magazine*, Vol. 45, No. 1, 38–57, Feb. 2003.
2. James, J. R. and P. S. Hall, eds., *Handbook of Microstrip Antennas*, Peter Peregrinus, UK, 1989.
3. Pozar, D. M. P. and D. H. Schaubert, *Microstrip Antennas, the Analysis and Design of Microstrip Antennas and Arrays*, Wiley-IEEE Press, New York, NY, 1995.
4. Mandelbrot, B. B., *The Fractal Geometry of Nature*, W. H. Freeman and Company, 1983.
5. Cohen, N., "Fractal antennas," *Communications Quarterly*, 9, 1995.
6. Shukla, B. K., N. Kashyap, and R. K. Baghel, "Wide slot antenna with Y shape tuning element for wireless applications," *Progress In Electromagnetics Research M*, Vol. 59, 45–54, 2017.
7. Mirzapour, B. and H. R. Hassani, "Size reduction and bandwidth enhancement of snowflake fractal antenna," *IET Microwave Antennas Propagation*, Vol. 2, No. 2, 180–187, 2008.



8. Suganthi, S., S. Raghavan, D. Kumar, and S. Hosimin Thilagar, "Planar fractal antennas for wireless devices," *IEEE 3rd International Conference on Electronics Computer Technology (ICECT 2011)*, VI-98–102, Kanyakumari, Apr. 8–10, 2011.
9. Ismahayati, W., P. J. Soh, R. Hadibah, and G. A. E. Vandenbosch, "Design and analysis of a multiband Koch fractal monopole antenna," *IEEE International RF and Microwave Conference*, 58–62, Seremban, Malaysia, Dec. 12–14, 2011.
10. Choukiker, Y. K., S. K. Sharma, and S. K. Behera, "Hybrid fractal shape planar monopole antenna covering multiband wireless communications with MIMO implementation for handheld mobile devices," *IEEE Transactions on Antennas and Propagation*, Vol. 62, No. 3, 1483–1488, Mar. 2014.
11. Wu, P., Z. Kuai, and X. Zhu, "Multi-band antennas comprising multiple frame printed dipoles," *IEEE Transactions on Antennas and Propagation*, Vol. 57, No. 10, 3313–3317, Oct. 2009.
12. Li, J., T. Jiang, and C. Cheng, "Hilbert fractal antenna for UHF detection of partial discharges in transformers," *IEEE Transactions on Dielectrics and Electrical Insulation*, Vol. 20, No. 6, 2017–2025, Dec. 2013.
13. Azari, A., A. Ismail, A. Sali, and F. Hashim, "A new super wideband fractal monopole dielectric resonator antenna," *IEEE Antennas and Wireless Propagation Letters*, Vol. 12, 1014–1016, 2013.
14. Baliarda, C. P., J. Romeu, and A. Cardama, "The Koch monopole: A small fractal antenna," *IEEE Transactions on Antennas and Propagation*, Vol. 48, No. 11, 1773–1781, Nov. 2000.
15. Oraizi, H. and S. Hedayati, "Miniaturization of microstrip antennas by the novel application of the giuseppe piano fractal geometries," *IEEE Transactions on Antennas and Propagation*, Vol. 60, No. 8, 3559–3567, Aug. 2012.
16. Dhar, S., R. Ghatak, B. Gupta, and D. R. Poddar, "A wideband Minkowski fractal dielectric resonator antenna," *IEEE Transactions on Antennas and Propagation*, Vol. 61, 2895–2903, 2013.
17. Dhar, S., K. Patra, R. Ghatak, B. Gupta, and D. R. Poddar, "A dielectric resonator-loaded Minkowski fractal-shaped slot loop hepta band antenna," *IEEE Transactions on Antennas and Propagation*, Vol. 63, No. 4, 1521–1529, 2015.
18. Borja, C. and J. Romeu, "On the behavior of Koch island fractal boundary microstrip patch antenna," *IEEE Transactions on Antenna and Propagation*, Vol. 51, No. 6, 1281–1291, Jun. 2003.
19. Puente-Baliarda, C., J. Romeu, R. Pous, and A. Cardama, "On the behavior of the sierpinski multiband fractal antenna," *IEEE Transactions on Antenna and Propagation*, Vol. 46, No. 4, 517–524, Apr. 1998.
20. Srivatsun, G. and S. Subha Rani, "A compact multiband fractal cantor antenna for wireless application," *European Journal of Scientific Research*, Vol. 71, No. 2, 273–282, 2012.
21. Srivatsun, G. and S. Subha Rani, "A novel compact multiband fractal antenna for wireless application," *International Journal of Microwave and Optical Technology*, Vol. 7, No. 2, 82–88, 2012.
22. Viti, L., A. Politano, and M. S. Vitiello, "Black phosphorus nanodevices at terahertz frequencies: Photo detectors and future challenges," *APL Materials*, Vol. 5, 035602, 2017.
23. Mitrofanov, O., L. Viti, E. Dardanis, M. C. Giordano, D. Ercolani, A. Politano, L. Sorba, and M. S. Vitiello, "Near-field terahertz probes with room-temperature nano detectors for sub wavelength resolution imaging," *Sci. Rep.*, Vol. 7, 44240, 2017.
24. Viti, L., J. Hu, D. Coquillat, A. Politano, W. Knap, and M. S. Vitiello, "Efficient Terahertz detection in black-phosphorus nano-transistors with selective and controllable plasma-wave, bolometric and thermoelectric response," *Sci. Rep.*, Vol. 6, 20474, 2016.
25. Viti, L., D. Coquillat, A. Politano, K. A. Kokh, Z. S. Aliev, M. B. Babanly, O. E. Tereshchenko, W. Knap, E. V. Chulkov, and M. S. Vitiello, "Plasma-wave Terahertz detection mediated by topological insulators surface states," *Nano Lett.*, Vol. 16, 80, 2016.
26. Viti, L., J. Hu, D. Coquillat, W. Knap, A. Tredicucci, A. Politano, and M. S. Vitiello, "Black-phosphorus Terahertz photo detectors," *Adv. Mater.*, Vol. 27, 5567, 2015.
27. Li, D. and J.-F. Mao, "Koch-like sided Sierpinski gasket multifractal dipole antenna," *Progress In Electromagnetics Research*, Vol. 126, 399–427, 2012.

28. Li, D. and J.-F. Mao, "Sierpinski-like Koch-like sided multifractal dipole antenna," *Progress In Electromagnetics Research*, Vol. 130, 207–224, 2012.
29. Karli, R. and H. Ammor, "A simple and original design of multiband microstrip patch antenna for wireless communication," *IJMA*, Vol. 2, No. 2, 41–44, 2013.
30. Azaro, R., L. Debiassi, E. Zeni, M. Benedetti, P. Rocca, and A. Massa, "A hybrid pre fractal three-band antenna for multi standard mobile wireless applications," *IEEE Antennas Wireless Propagation Letter*, Vol. 8, 905–908, 2009.